

# Sol-Gel Synthesis and Characterization of Carbon doped TiO<sub>2</sub> based on *Solanum Tuberosum* Starch

Diandari Siti Nur Ichسانی\*, Cahyorini Kusumawardani

\* Department of Chemistry, Universitas Negeri Yogyakarta

---

## Article Info

### Article history:

Received Nov 12<sup>th</sup>, 2021

Revised Dec 10<sup>th</sup>, 2021

Accepted Dec 26<sup>th</sup>, 2021

### \*Corresponding Author:

Diandari Siti Nur Ichسانی  
Department of Chemistry Education  
Universitas Negeri Yogyakarta

Email:  
diandarisiti.2017@student.uny.ac.id

## ABSTRACT

The carbon-doped TiO<sub>2</sub> have been synthesized through sol-gel method using *Solanum tuberosum* starch as carbon source. The carbon precursor composition and reaction time were varied to study its influence to the crystal structure and electronic structure of resulted material. The C- TiO<sub>2</sub> product was characterized by XRD, UV-Vis DRS, FTIR, and photocatalytic activity examine by methylene blue degradation. The results showed that variations in the composition of the carbon precursor and reaction time affected the characteristics of the crystal structure and photocatalyst activity of C- TiO<sub>2</sub>. The optimum variation was found in the variation of 1.5 gram carbon composition and 24 hours hydrolysis time which had the smallest particle size and lowest bandgap energy. The highest photocatalyst activity was obtained at a 24-hour reaction time variation with 59.375% percent of methylene blue degraded in the second-order reaction with a k value of 2.1351.

**Keywords:** C-TiO<sub>2</sub>, Sol-gel, Potato Starch, Photocatalyst, Methylene Blue Degradation

---

## 1. INTRODUCTION

Industrialization is closely related to economic growth, yet the process raises byproducts in hazardous waste (Bottero, *et al.*, 2011). Liquid waste is often discharged without treatment into the environment. Waste that is difficult to degrade will accumulate and endanger aquatic biota by reduces the level of dissolved oxygen in the water and inhibits the photosynthesis of aquatic plants (Veliev *et al.*, 2006), such as dyes material (Aliah and Karlina, 2015) that found with an average waste concentration in the water 300 mg/L (Sahoo, C., *et al.*, 2012). Photocatalysts can be an effective alternative for handling aquatic waste (Suchaya, *et al.*, 2016). The working principle of photocatalysts to decompose waste is that sunlight excites electrons in photocatalyst compounds and produces hydroxyl radicals which will react redox to decompose pollutants (Mano, T., *et al.*, 2015). The performance of the photocatalyst is determined by the light received and the semiconductor used (Bey, Sirhan, 2009). TiO<sub>2</sub> is a safe and environmentally friendly semiconductor compound (Sudha, D., and Silvakumar, P., 2015), high thermal and chemical stability, inert, non-toxic, high surface area, easy to prepare, and it has a large bandgap (Yan, Li, & Xia, 2017). TiO<sub>2</sub> has a bandgap at 3.2 eV and active in the ultraviolet (UV) region (Rajaraman, Parikh, & Gandhi, 2019). The weakness of TiO<sub>2</sub> was its active region in the ultraviolet range because only 5% of UV light reaches the earth's surface and unspecified (Day, 2009).

Efforts have been made to shift TiO<sub>2</sub> absorption into visible light, including structural modification, reduction, doping of metal compounds, and doping of non-metallic compounds (Yan, Li, & Xia, 2017). Doping of non-metallic compounds shows a shift in TiO<sub>2</sub> absorption to the visible area, does not cause impurities (Ullatil & Soumya B. Narendranath, 2018). One of the non-metallic compounds used is carbon. Carbon has a better ability to join the TiO<sub>2</sub> lattice structure (Rasoulnezhad, Kavei, Ahmadi, & Rahimpour, 2017). Cellulose and starch can be alternative sources of carbon that are environmentally friendly (Kumar, Singh, & Singh, 2008).

Various methods can be used for doping TiO<sub>2</sub> by natural ingredients. Sol-gel is the most frequently used (Purwiandono & Kartini, 2016). Sol-gel has a simple operation and equipment, and no special conditions are required because the reaction occurs at room temperature and atmospheric pressure. Sol-gel was easy, inexpensive, and produced high-purity products (Ovodok, *et al.*, 2018).

## 2. RESEARCH METHOD

In this study, the researchers were conducted at the Chemical Research Laboratory, FMIPA UNY, and the samples were characterized at the UII Chemistry Laboratory (UV-Vis DRS and FTIR), UNY Integrated Laboratory (UV-Vis DRS and XRD) from February to May 2021. Focus on research is the effect of dopant precursor mass variation (carbon) and reaction time variation on the synthesis and characterization of C- TiO<sub>2</sub>. Synthesis was carried out by dissolving potato starch as much as 0.5 grams, 1 gram, and 1.5 grams in 80 mL absolute ethanol, then homogenized and added TTIP 3 mL dropwise. Next, build an acidic atmosphere by adding 5 mL of glacial acetic acid, hydrolysis on sol-gel for 24 hours, and aging for 24 hours. The gel phase was then filtered and calcined at a temperature of 500°C. The best XRD and UV results were then taken as the mass of carbon precursors used for variations in hydrolysis time. Variation of hydrolysis time using the same steps by changing the hydrolysis time in the sol-gel process to 6 hours, 12 hours, and 24 hours. The synthesis results were then characterized using FTIR, UV-Vis DRS, and XRD.

## 3. RESULTS AND ANALYSIS (10 PT)

The synthesis of C- TiO<sub>2</sub> with carbon dopants from potato starch obtained a white powder before calcination and a grayish-white powder after the calcination process. The synthesized compounds were analyzed using FTIR before and after calcination, XRD instruments, UV-Vis DRS, and photocatalyst activity test by methylene blue degradation.

### 3.1. FTIR Analysis

The analysis wavelength was taken from 400cm<sup>-1</sup> to 4,000cm<sup>-1</sup>. Analysis of the results with IR spectrophotometer in this study aims to determine the success of doping and determine the functional groups after calcination. The results of the IR spectrophotometer are in **Figure 1.** and **Table 1.**

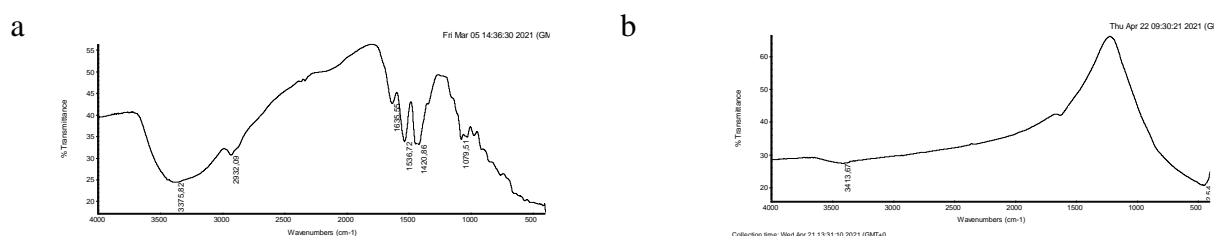


**Figure 1.** Infrared vibration spectra a) before calcination, b) after calcination

**Table 1.** Infrared vibration before and after calcination

Before calcination		Sesudah kalsinasi	
Wavelength (cm <sup>-1</sup> )	Vibration	Wavelength (cm <sup>-1</sup> )	Vibration
1635,55	Bending Ti-OH	452	Vibration of Ti-O
1079,51	Stretching C-O	1542,8	Stretching C-O-O
1420,88	Bending C-O	3413,57	Stretching O-H
1538,72	Stretching C-C		
2932,09	Stretching -CH		
3375,82	Stretching -OH		

From the IR spectra data above, the carbon vibrations in stretching C-O at 1079.51 cm<sup>-1</sup>, bending C-O at 1420.88 cm<sup>-1</sup>, stretching C-C at 1538.72 cm<sup>-1</sup>, and stretching C-H at 2932.09 cm<sup>-1</sup> indicated the presence of carbon on the synthesized compound. Stretching and bending of C-O is assumed to be carbon doped at the interstitial position of the lattice of TiO<sub>2</sub>. The presence of C-C and C-H bonds indicates that not all of the carbon were doped in the TiO<sub>2</sub> crystal lattice but rather accumulates in one position and forms bulk (Di Valentin, *et al.*, 2005). Therefore, the undoped carbon were then removed by calcination. After calcination, it is assumed that the undoped carbon group was missing, as evidenced by the absence of C-C and C-H absorption. The absorption in the 1542 cm<sup>-1</sup> region indicates the presence of carbon absorption from the COO- group, means that the carbon is doped on the crystal lattice and forms bonds with the O atom next to it (Pambudi, *et al.*, 2018). Ti-O absorption at 452 cm<sup>-1</sup> showed that the carbon was doped interstitially and does not replace oxygen to form Ti-C. According to the experimental results of Di Valentin, *et al.*, (2005) that carbon tends to bond with other carbons to form double bonds or bind oxygen atoms compared to Ti. The stretching and bending of -OH is assumed to be a water molecule that sticks after the synthesis was completed.

### 3.2. XRD Analysis

The X-Ray Diffraction (XRD) instrument used in this study is the Rigaku X-Ray Diffraction operated at 2θ between 2° to 80° using a Cu-K radiasi radiation source (1,540593Å). The diffractogram of the mass variation of the carbon precursor and the variation of the reaction time can be seen in **Figure 2**.

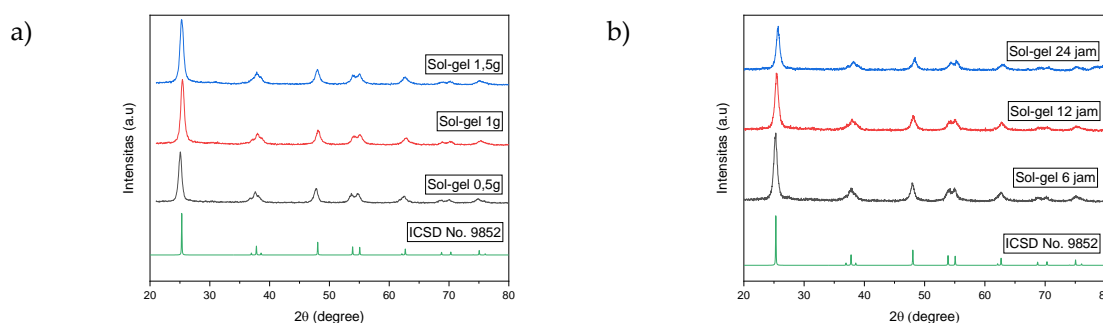


**Figure 2.** XRD diffractogram a) precursor mass ratio variation, b) time reaction variation

There was a shift in the diffraction pattern of the carbon precursor mass variation towards the smaller 2θ, indicates the presence of carbon doping in TiO<sub>2</sub> compounds (Habibbi and Hoursshidi, 2019). The carbon precursor composition variation also shows the higher intensity with increasing mass of the dopant. Peaks in the variation of reaction time showed a shift towards greater 2θ, but being around the peak (101) anatase. The anatase peak in JCPDS 01-073-1764 was at 2θ 25.367° (101); 37.909° (004); 48.158° (200); 54.051° (105); 55.204° (211); 63.13 (204) 70.479° (220); and 75.227° (215). The longer the reaction time, the lower the peak intensity, indicating a phase transformation will occur. Research conducted by Jannah (2019) reported that the addition of a carbon precursor mass encourages the growth of the rutile phase because the interfacial tension affects crystal growth (Li,

*et al.*, 2007). The relationship of typical anatase diffraction angle, FWHM, and particle size calculated by the Debye Scherrer equation is presented in **Table 2**.

**Table 2.** Table of diffraction angle, FWHM, and particle size

Carbon mass precursor variation					Reaction times variation						
	2 $\theta$	hkl	FWHM	D (nm)	Rerata D (nm)		2 $\theta$	hkl	FWHM	D (nm)	Rerata D (nm)
0,5 grams	25,05	101	0,73	10,98	9,98	6 Hours	25,25	101	0,79	10,36	10,72
	37,65	004	1,52	5,52			37,85	004	1,44	5,81	
	47,76	200	0,81	10,77			47,98	200	0,79	10,97	
	54,77	105	0,88	10,15			53,97	105	0,88	10,17	
	69,98	220	0,78	12,48			70,13	220	0,59	16,27	
1,0 gram	25,36	101	0,78	10,41	9,74	12 hours	25,45	101	0,84	9,74	9,39
	38,03	004	1,61	5,22			38,03	004	1,65	5,08	
	48,13	200	0,91	9,59			48,14	200	0,92	9,48	
	54,05	105	0,84	10,61			54,09	105	0,85	10,47	
	70,03	220	0,76	12,86			70,29	220	0,79	12,23	
1,5 grams	25,31	101	0,81	10,09	8,98	24 hours	25,67	101	0,80	10,18	8,83
	37,9	004	1,56	5,37			38,22	004	1,51	5,57	
	47,99	200	0,91	9,55			48,34	200	0,88	9,95	
	55,01	211	0,98	9,12			54,37	105	0,93	9,57	
	75,19	215	0,93	10,76			62,97	204	1,05	8,88	

The synthesized C- TiO<sub>2</sub> has nanocrystals because it is much smaller than 100 nm. From the calculation results, the mass of 1.5 grams of carbon precursor and the hydrolysis reaction time of 24 gave the smallest crystal size. From the results table, it can be seen that the more carbon precursors are added, the smaller the particle size obtained. The results of computational research can explain the smaller particle size along with the increase in carbon doping by Di Valentin, *et al.*, (2005), who showed that on carbon doping, carbon compounds tend to form double bonds between carbon or bond to O atoms rather than bonding to Ti so that carbon tends to be doped in interstitial positions. In the interstitial position, carbon is assumed to be bonded to 3 oxygen atoms. Ti-O bond length is 1.992-2.002Å, while the interstitial C-O bond length is 1.416-1.432Å. The increase in doped carbon will further increase the number of shorter C-O bonds than Ti-O bonds, thus allowing distortion to occur, resulting in smaller crystals. The presence of carbon in the middle of the TiO<sub>2</sub> lattice does not have much effect or increase the crystal size because the size of carbon is relatively small compared to Ti. The possibility of substitution of oxygen by carbon to form Ti-C can be ruled out because the Ti-C bond is weaker and longer than Ti-O, so it will give a larger size.

Table 2 showed that the size decreases with reaction time. This is consistent with the theory of collisions between molecules that says the longer the reaction time, the more the possibility of collisions between particles can occur where the reaction takes place more perfect (Mao, 2005). The perfect sol-gel process will give a small and uniform size. The particle size is inversely proportional to the resulting surface area (Manique, *et al.*, 2017), in the synthesis of nanoparticles the smaller the particles obtained indicate the possibility of a larger surface area. Therefore, the results obtained by XRD refinement are the most effective results on the mass variation ratio of 1.5 grams of carbon precursors and reaction time of 24 hours.

### 3.3. UV-Vis DRS Analysis

The C- TiO<sub>2</sub> compound was characterized by UV-Vis DRS at a wavelength of 200-800nm to determine the band gap energy and absorption region of the synthesized compound. The following data shows the bandgap energy using the Tauc Plot equation were shown in Figure 3.

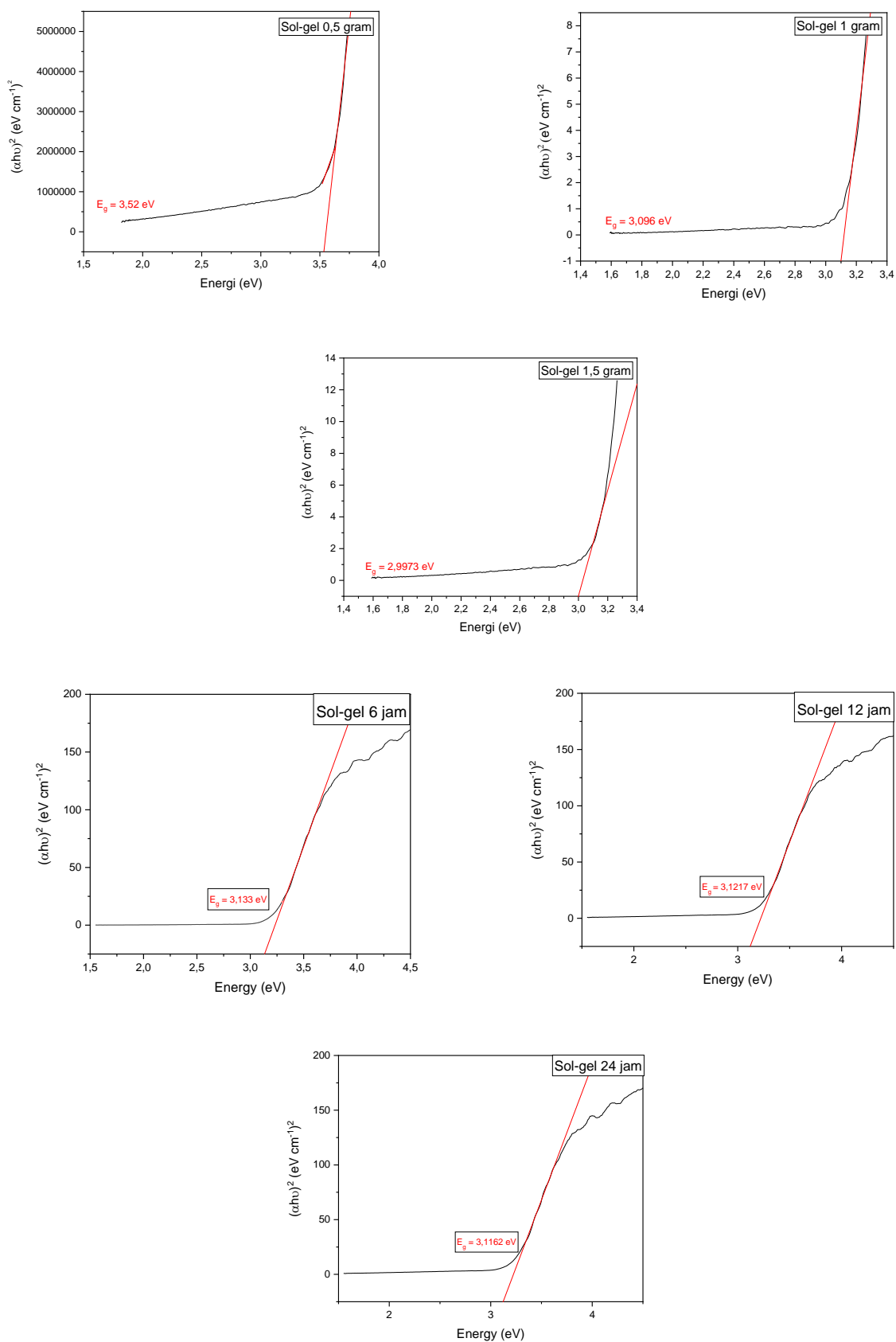


Figure 4. Bandgap energy by *Tauc plot* equation

From **Figure 4**, it can be seen that variations in the mass of the carbon precursors cause differences in the band gap energy. The more variations in the mass of the carbon precursor, the smaller the band gap energy. The best results were obtained at the smallest band gap energy, namely the mass of 1.5 grams of carbon precursor. The indirect wavelength ( $\lambda$ ) or called ( $\lambda_{bg}$ ) can be calculated by the equation  $E_g = 1240/\lambda$ , so that the maximum indirect wavelength data ( $\lambda_{bg}$ ) is obtained in **Table 3**.

**Table 3.** Maximum wavelength of carbon mass precursor variation

Carbon mass precursor variation (grams)	$\lambda_{bg}$ (nm)
0,5	352
1,0	401
1,5	414

The addition of carbon precursor mass shows a shift towards a larger wavelength (red shift). The electronic transition of  $\pi$  to  $\pi^*$  occurs at a wavelength of 200-400nm (UV). The electronic transition of  $n$  to  $\pi^*$  occurs at a wavelength of 401-700nm (Visible). Based on the **Table 3**, C- TiO<sub>2</sub> synthesized with 0.5 gram carbon variation has  $\pi$ - $\pi^*$  electronic transition, while 1.0 gram and 1.5 gram carbon variation has  $n$ - $\pi^*$  electronic transition.

From **Figure 4**, it is obtained that the band gap energy decreases with the hydrolysis time. So from the analysis using UV-DRS obtained the best results with the smallest band gap energy, namely the hydrolysis reaction for 24 hours. UV-Vis absorbance data vs. the wavelength DRS will provide data on the maximum absorbance of compound C- TiO<sub>2</sub>. In the experiment of the hydrolysis reaction time variations obtained in **Figure 5**.

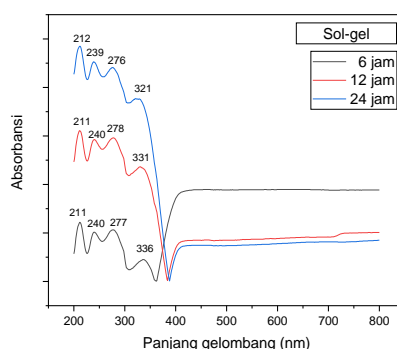


**Figure 5.** Maximum absorbance of hydrolysis reaction time variations

**Figure 5**, shows the longer the reaction time, the shift towards UV (blue shift) with a 24-hour wavelength variation that is closest to the visible area. This shows that the synthetic C-TiO<sub>2</sub> is active in the UV region. The electron transition that may occur is the  $\pi$  to  $\pi^*$  transition because this transition is at a wavelength of 200-400nm.

#### 4. CONCLUSION

Based on this research can be concluded that variations in the mass of carbon precursors and reaction time variation affects the crystal structure, particle size, electronic structure, and photocatalytic activity. Results obtained at the best synthesis of the mass variation of 1.5 gram and 24-hour reaction time with the band gap energy of successive 2.9937 eV and 3.1162 eV.

## REFERENCES

- Aliah, H., & Karlina, Y. (2015). Semikonduktor TiO<sub>2</sub> sebagai material fotokatalis berulang. *Jurnal Istek*, 9(1).
- Bey, Sirha. (2009). Pengujian Kinerja Fotokatalis Berbasis TiO<sub>2</sub> Untuk Produksi Hidrogen dari Air. *Jurnal Skripsi*. Jakarta : Fakultas Teknik Program Studi Teknik Kimia
- Bottero, M., Comino, E., & Riggio, V. (2011). Application of Hierarchy Process and The Analytic Network Process for The Assessment of Different Wastewater Treatment Systems. *Environmental modelling & software*, 26(10), 1211-1224.
- Day, E. D., Pink, J. D., & Knight, R. B. (2009). *U.S. Patent Application No. 11/835,899*.
- Day, R A, dan Underwood, A L., (2002), Analisis Kimia Kuantitatif Edisi Keenam. Jakarta : Erlangga
- Di Valentin, C., Pacchioni, G., & Selloni, A. (2005). Theory of carbon doping of titanium dioxide. *Chemistry of Materials*, 17(26), 6656-6665.
- Habibi, S., & Jamshidi, M. (2020). Sol-gel synthesis of carbon-doped TiO<sub>2</sub> nanoparticles based on microcrystalline cellulose for efficient photocatalytic degradation of methylene blue under visible light. *Environmental technology*, 41(24), 3233-3247.
- Jannah, S. N. (2019). *Sintesis dan karakterisasi TiO<sub>2</sub>/Karbon aktif menggunakan metode Sol-gel* (Doctoral dissertation, Universitas Islam Negeri Maulana Malik Ibrahim).
- Kumar, R., Singh, S., & Singh, O. V. (2008). Bioconversion of lignocellulosic biomass: biochemical and molecular perspectives. *Journal of industrial microbiology and biotechnology*, 35(5), 377-391.
- Li, Y., Zhang, S., Yu, Q., & Yin, W. (2007). The effects of activated carbon supports on the structure and properties of TiO<sub>2</sub> nanoparticles prepared by a sol-gel method. *Applied Surface Science*, 253(23), 9254-9258.
- Maddu, A. (2009). Pengaruh Konsentrasi Awal dan Penambahan H<sub>2</sub>O<sub>2</sub> terhadap Efektivitas Degradasi Fotokatalisis Metilen Biru pada Film TiO<sub>2</sub>. *Jurnal Purifikasi*, 10(1), 71-78.
- Manique, M. C., Silva, A. P., Alves, A. K., & Bergmann, C. P. (2017). Titanate nanotubes produced from microwave-assisted hydrothermal synthesis: characterization, adsorption and photocatalytic activity. *Brazilian Journal of Chemical Engineering*, 34(1), 331-339.
- Mano, T., Nishimoto, S., Kameshima, Y., & Miyake, M. (2015). Water treatment efficacy of various metal oxide semiconductors for photocatalytic ozonation under UV and visible light irradiation. *Chemical Engineering Journal*, 264, 221-229.
- Mao, Y., Park, T. J., & Wong, S. S. (2005). Synthesis of classes of ternary metal oxide nanostructures. *Chemical communications*, (46), 5721-5735.
- Ovodok, E., Maltanova, H., Poznyak, S., Ivanovskaya, M., Kudlash, A., Scharnagl, N., & Tedim, J. (2018). Sol-gel Template of Mesoporous carbon-dopes TiO<sub>2</sub> with Photocatalytic Activity under Visible Light. *Materials Today*. Elsevier.
- Pambudi, A. B., Kurniawati, R., Iryani, A., & Hartanto, D. (2018, December). Effect of calcination temperature in the synthesis of carbon doped TiO<sub>2</sub> without external carbon source. In *AIP Conference Proceedings* (Vol. 2049, No. 1, p. 020074). AIP Publishing LLC.
- Purwiandono, G., & Kartini, I. (2016). Synthesis Of Porous TiO<sub>2</sub> With Starch Template And Its Photoactivity Towards Photodegradation Of Methylene Blue. *EKSAKTA: Journal of Sciences and Data Analysis*, 15(1-2), 1-13.
- Rajaraman, T. S., Parikh, S. P., & Gandhi, V. G. (2020). Black TiO<sub>2</sub>: A review of its properties and conflicting trends. *Chemical Engineering Journal*, 389, 123918.
- Rasoulnezhad, H., Kavei, G., Ahmadi, K., & Rahimpour, M. R. (2017). Combined sonochemical/CVD method for preparation of nanostructured carbon-doped TiO<sub>2</sub> thin film. *Applied Surface Science*, 408, 1-10.
- Sahoo, C., Gupta, A. K., & Pillai, I. M. S. (2012). Heterogeneous photocatalysis of real textile wastewater: evaluation of reaction kinetics and characterization. *Journal of Environmental Science and Health, Part A*, 47(13), 2109-2119.

- Sucahya, T. N., Permatasari, N., & Nandiyanto, A. B. D. (2016). Fotokatalis untuk pengolahan limbah cair. *Jurnal integrasi proses*, 6(2).
- Sudha, D., & Sivakumar, P. (2015). Review on the photocatalytic activity of various composite catalysts. *Chemical Engineering and Processing: Process Intensification*, 97, 112-133.
- Ullattil, S. G., Narendranath, S. B., Pillai, S. C., & Periyat, P. (2018). Black TiO<sub>2</sub> nanomaterials: a review of recent advances. *Chemical Engineering Journal*, 343, 708-736.
- Veliev, E. V., Öztürk, T., Veli, S. E. V. İ. L., & Fatullayev, A. G. (2006). Application of diffusion model for adsorption of azo reactive dye on pumice. *Polish Journal of Environmental Studies*, 15(2).
- Yan, X., Li, Y., & Xia, T. (2017). Black titanium dioxide nanomaterials in photocatalysis. *International Journal of Photoenergy*, 2017.